IEEE Access
Multidisciplinary | Rapid Review | Open Access Journal

Received April 23, 2018, accepted May 24, 2018, date of publication May 30, 2018, date of current version July 12, 2018.

Digital Object Identifier 10.1109/ACCESS.2018.2842106

A Force and Displacement Compensation Method Toward Divergence and Accuracy of Hardware-In-the-Loop Simulation System for Manipulator Docking

SIMIAO YU, JUNWEI HAN, ZHIYONG QU, AND YU YANG
Institute of Electrohydraulic Servo Simulation and Test System, Harbin Institute of Technology, Harbin 150001, China
Corresponding author: Zhiyong Qu (quzyhit@163.com)

This work was supported by the National Natural Science Foundation of China under Grant 51475116.

ABSTRACT The hardware-in-the-loop (HIL) simulation system for manipulator docking is an important means to simulate the flexible manipulator on-orbit docking dynamics process. However, the delay of the HIL simulation system leads to the accuracy loss and divergence problems of the system; in this paper, a force and displacement compensation method was proposed toward these problems of the manipulator docking HIL simulation system for single-mass, multi-stiffness, and multi-damping contact. First, time delays including the contact force delay and the force measurement delay were considered. The real-time on-line identification method was applied in the time-varying HIL simulation system, and the contact force delay was compensated by the identification parameters and the discrete force compensation model. The force measurement delay was compensated by a phase lead based force compensation model. The dynamic response model of the motion simulator was not required in the force compensation. In addition, the displacement phase lead compensation model was used to reduce the displacement phase delay of the motion simulator, which improved the reproduction accuracy of the HIL simulation system. Based on the simulation and experimental results, it is shown that the proposed method can effectively and satisfactorily prevent the divergence and improve the accuracy of the reproduction.

INDEX TERMS Manipulator docking, hardware-in-the-loop simulation, contact force delay, force measurement delay, displacement phase delay, force and displacement compensation.

I. INTRODUCTION

ITH development of the space exploration, the research on the on-ground simulation technology of the space manipulator docking is particularly important. The terminal of the manipulator is equipped with an end-effector, which uses the docking mechanism (DM) to achieve capture, drag and other docking operations on the target-adapter equipped on the spacecraft. Due to the high cost and important task, the DM, docking initial condition and strategy must pass the verification on the ground before the spacecraft launches. Thus, accurate simulation of the docking dynamics process on the ground is the premise for designing and analyzing the DM, as well as for the on-orbit servicing such as manipulator docking and space station construction [1]–[3].

The docking simulation of the space manipulator should be carried out under the condition of zero gravity (zero-g) to simulate the weightlessness of the real outer space [4], [5]. At present, the HIL simulation is most often used, for it combines the fidelity of the physical simulation and the flexibility of the numerical simulation. The motion of the spacecraft in the zero-g space is calculated from a numerical model and then reproduced by a robotic motion simulator. The actual contact force is produced from the real DM. The HIL simulation system for manipulator docking has three main forms based on the state of the manipulator: (1) The manipulator is a physical object. The HIL simulation system needs to simulate the docking dynamics process of the manipulators with different stiffnesses, which causes that the experiment cost is high and the flexibility on changing objects is low. (2) The manipulator is a numerical model. Under this condition, the contact force of the HIL simulation system is determined by the contact stiffness and damping of

the DM. However, the stiffness of the DM is usually large; in this case, the HIL simulation system with a delay is easy to diverge [6]–[8]. The divergence problem of the system is difficult to be completely solved because of the complex collision principle, the uncertain delay of the motion simulator and the HIL simulation system with multi-degree-of-freedom (multi-DOF); thus, the high stiffness contact should be avoid in the experiment. (3) The manipulator is equivalent to a six-DOF physical spring. In order to prevent the adverse effects of a large overall motion at the end of the manipulator on the docking, each joint of the manipulator in the docking process is in a locking state [9]; therefore, the manipulator in the docking process is represented by the elastic deformation, so the manipulator can be equivalent to a six-DOF mass-stiffness-damping system [6], [10]. The equivalent stiffness of the manipulator can be introduced into the HIL simulation system by designing a six-DOF physical spring mechanism. In view of the low stiffness of the spring mechanism (manipulator), the stiffness of the system can be reduced, and the stability of the system can be improved; this form of the HIL simulation system reduces the cost and guarantees the flexibility on changing the objects. In this paper, the third form of the HIL simulation system for manipulator docking is chosen as the research object. The serial-type robots are developed as the HIL motion simulator to simulate the contact dynamics in space [11]–[13]. In this study, the parallel-type robot will be used as the motion simulator. Its high stiffness, high precision and high payload are beneficial to simulate the motion state of a spacecraft.

One challenging problem for the HIL simulation is the divergence and accuracy loss. The dynamic response delay of the motion simulator makes the actual position of the motion simulator deviate from the desired position of the dynamics calculation and results in the actual force measured by the sensor deviates from the desired force corresponding to the desired position (which is called the contact force delay). After cyclic calculation and measurement, the displacement deviation of motion simulator and the deviation of the force measurement increase; which not only affect the accuracy of system reproduction, but also often cause the system divergence, resulting in the damage of the DM.

Several methods of delay compensation for HIL simulation system have been put forward. (1) When the delay model is known and time-invarying, the model-based forward compensation method can be applied. Chang *et al.* [14] considered the delay of the electrical components and digital control; and developed a compensation model based on the quantitative feedback theory (QFT); but design of the proper parameters was not easy. Shimoji *et al.* [15] applied a first-order compensation model aiming at the pure or first-order time delay, which decreased the delay of the simulator. Osaki *et al.* [16] and Abiko *et al.* [17] used force compensation method to achieve the desired contact force by adding the virtual force onto the measured force, respectively; the research objects were undamped contact systems, and the contact frequency and time delay were known. (2) When the delay model is unknown, the compensation method becomes difficult and immature. Ananthakrishnan *et al.* [18] developed a prediction-based feed forward filter to make a ground-based hydraulic simulator generate contact forces and rebound velocities that matched those desired during Shuttle on-orbit berthing operations; however, the prediction model was trained offline, the on-orbit data for the training was unknown before the simulation. Zebenay *et al.* [19] used the virtual damper force to compensate the measured force; although the delay model for the motion simulator wasn't needed, this method required a large number of experiments and experiences to modify the model and parameters. The force compensation method was studied for the delay of the elastic contact system by Qi *et al.* [20]; the measured force was compensated through the force compensation model based on the stiffness identification, and the stability of the system was improved; however, the method was strictly limited to the form of contact and didn't consider the response compensation of the motion simulator.

The primary cause for the divergence and accuracy loss of the HIL simulation system is the delay which results in the deviation of the displacement and the contact force. However, the motion simulator has different delay characteristics at different positions and frequencies, so it is difficult to completely eliminate the dynamic response delay. In the literature, the dynamic response delays of the motion simulator or the contact force delays are compensated and corrected through predictions and experiments, but these methods are tedious and prone to bias. In this paper, a method combining force and displacement compensations is proposed to prevent the divergence and accuracy loss of the manipulator HIL simulation system. The contact force compensation method is based on model-free compensation, and the displacement phase compensation method is model-based compensation. Force compensation ensures that the force input to the dynamics model is the same as the desired force corresponding to the desired position, which prevents the system from diverging. The displacement phase compensation is used to further improve the accuracy of the reproduction of the desired displacement. Compared with the current research, the main contributions of this study are as follows:

(1) The physical objects and contact form in the HIL simulation system are different. The current literature basically aims at two rigid spacecrafts docking; the contact force is determined by the single contact stiffness and the single contact damping during the HIL simulation system docking. In this study, a space manipulator (i.e. six-DOF spring mechanism) and an end-effector are the physical objects, five attribute parameters of the double-stiffness (manipulator and contact stiffness), the double-damping (manipulator and contact damping), and the single-mass (effective mass of the end-effector and the manipulator) influence the contact force during the docking, making the contact form and the force compensation method become complicated.

(2) The force compensation is based on the multi-parameter on-line identification. Five attribute parameters are time-varying in the docking process. In order to get the accurate compensation force, the real-time on-line identification parameters method is adopted, and the compensation force is calculated by the deviation between the input and output displacement of the motion simulator. Moreover, the phase lead compensation model is used to compensate the sensor's measurement delay.

(3) The force compensation model is established in the discrete-time domain instead of the usual continuous-time domain. Identification is usually carried out in a discrete-time domain. In this study, the identification results of a complex contact force model after discretization are five process parameters determined by the attribute parameters. The attribute parameters can be calculated through the process parameters, but the results have a numerical singular problem, which leads to the distortion compensation. Therefore, a discrete-time domain force compensation model of the process parameters is used to calculate the compensation force.

(4) The displacement phase lead compensation model is established based on dynamics frequency. Although it is difficult to eliminate the delay of the motion simulator, the dynamics frequency range of the docking can be estimated in advance through the simulation parameters; therefore, phase lead compensation model can be established to reduce the motion simulator's phase delay in the dynamics frequency range and improve the reproduction accuracy.

This paper consists of six sections. Following this section of the introduction, the HIL simulation system for manipulator docking is introduced in section II. The model of the HIL simulation system is described in section III. Compensation models of HIL simulation system for manipulator docking are proposed in section IV. Simulations and experiments are included in Section V. Finally, section VI gives the conclusion.

II. HIL SIMULATION SYSTEM FOR MANIPULATOR DOCKING

A. MANIPULATOR DOCKING SYSTEM

Figure 1 shows the space docking system, which has a spacecraft, a target-adapter, an end-effector, a manipulator and a space station (the mass of the space station is huge, so that its displacement under the docking force is negligible, and it is regarded as a stationary object during the docking). The success of the docking depends on the relative position of the end-effector and the target-adapter. Considering the elastic deformation of the manipulator, the manipulator can be regarded as two parts: a deformable flexible part (at the terminal of the end-effector, which can fully simulate the flexibility of the manipulator) and a non-deformable rigid part, so the rigid part of manipulator and the space station can be regarded as a static whole. During the docking, the end-effector moves under the actions of the flexible part and the contact force.

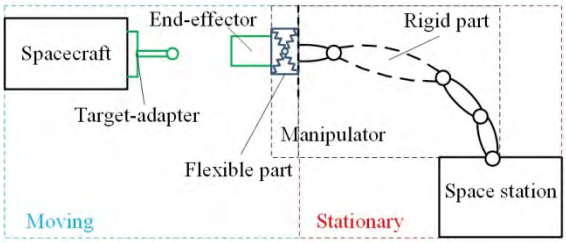

FIGURE 1. The manipulator docking system.

B. HIL SIMULATION SYSTEM FOR MANIPULATOR DOCKING

The structure of the HIL simulation system for manipulator docking is illustrated in Fig. 2. The physical objects include a force sensor, an end-effector, a six-DOF spring mechanism, a target-adapter, a six-DOF parallel robot (motion simulator) and a frame. The target-adapter and the end-effector used in the HIL simulation are the same as those in real space, which generate an actual contact force during the contact. The force sensor is attached under the frame, and the six-DOF spring mechanism is placed between the force sensor and the end-effector to simulate the flexible part of the manipulator in Fig. 1. A six-DOF parallel robot is used to reproduce the motion of the spacecraft for its high stiffness and accuracy. The dynamics model used in the HIL simulation describes the motion of the spacecraft with respect to the contact force measured by the force sensor. In the drag stage of manipulator docking, the zero-g space environment is simulated in the dynamics model.

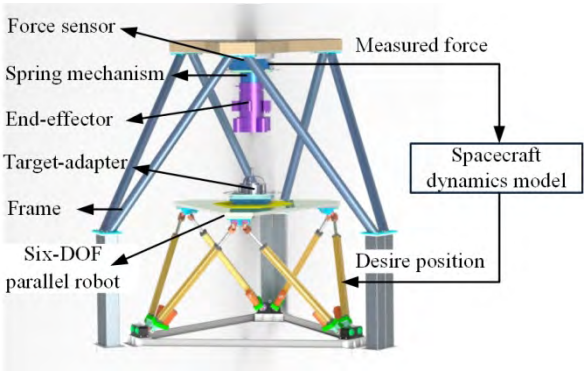

FIGURE 2. Structure of the HIL simulation system for manipulator docking.

The drag operation is realized by the drag mechanism which locates inside the end-effector. Schematic diagram of the drag mechanism and the drag principle is shown in Fig. 3. A lead screw is mounted inside the end-effector, and a motor drives the lead screw to rotate at a constant angular speed; the constant speed rotation of the lead screw can be transformed into a constant speed linear motion of the drag mechanism. Before the drag stage, three wire ropes of the drag mechanism have already captured and fixed the rod of the target-adapter; during the drag stage, the wire ropes move up with the drag

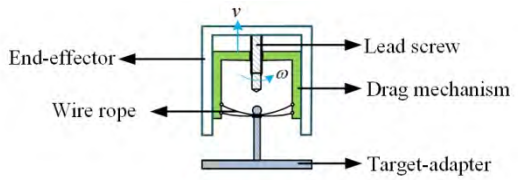

FIGURE 3. Schematic diagram of the drag mechanism and the drag principle.

mechanism, which makes the target-adapter move under the elastic forces produced by the deformation of the wire ropes.

C. PRINCIPLE OF THE HIL SIMULATION SYSTEM FOR MANIPULATOR DOCKING

The principles of the real space docking and the HIL simulation for manipulator docking are shown in Fig. 4 and Fig. 5, respectively. The physical elements of Fig. 5 are in bold words, and the parts performed by the software models of Fig. 5 are in non-bold words. The force sensor determines whether the HIL system can get actual contact force at the current moment, and the motion simulator determines whether the HIL system can reproduce the desired displacement to get the desired contact force at the next moment. When the dynamics model of the spacecraft can accurately describe the motion of the spacecraft; the closer the F' and x' of the HIL simulation system are to the F and x of the real docking system, and the higher the fidelity of the HIL simulation system is.

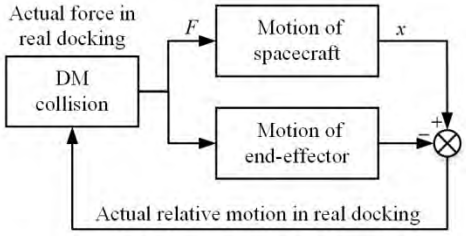

FIGURE 4. The principle of the real space docking.

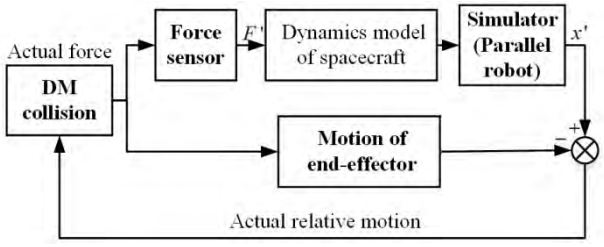

FIGURE 5. The principle of the HIL simulation for manipulator docking.

III. MODELING OF THE HIL SIMULATION SYSTEM FOR MANIPULATOR DOCKING

The model of the HIL simulation system is shown in Fig. 6, which is the prerequisite to establish the force and displacement compensation model.

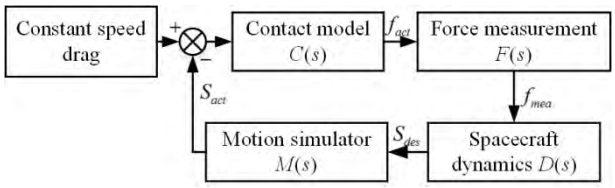

FIGURE 6. Model of the HIL simulation system.

A. SPACECRAFT DYNAMICS MODEL

The spacecraft moves under the elastic forces produced by the deformation of the wire ropes, and the flexible wire rope acts on the target-adapter can be regarded as a flexible spring with stiffness and damping acts on the target-adapter. The contact force is affected by the stiffness and damping of the wire rope in vertical direction, and the drag process is represented by a single-DOF motion. The interaction between the mechanisms can be described in Fig. 7. k_m and c_m are the stiffness and damping of the manipulator (six-DOF spring mechanism) in the vertical direction; k_p and c_p are the stiffness and damping of the wire rope in the vertical direction; v is the relative velocity (constant value) of the drag mechanism and the end-effector.

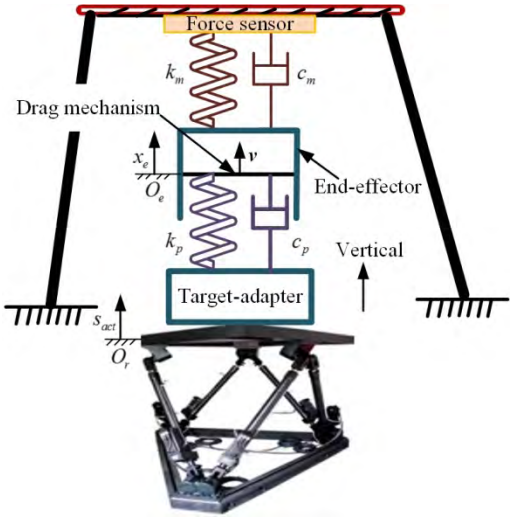

FIGURE 7. The interaction between the mechanisms in docking.

The mass of the end-effector m_e (no more than 100 kg) is very small relative to that of the spacecraft m_s (usually in a few tons or tens of tons) and the oscillation acceleration produced by the end-effector is small because of the small stiffness of the manipulator; then the inertia force of the end-effector is negligible for the dynamics characteristics of the spacecraft. The measured force f_{mea} is equal to the contact force, the dynamics model of the spacecraft is:

$$m_s \cdot d^2 s_{des}(t)/dt^2 = f_{mea}(t) \tag{1}$$

where s_{des} is the desired displacement of the dynamics calculation (input of the motion simulator).

Then, the transfer function of the dynamics is:

$$D(s) = 1/\left(m_s s^2\right) \tag{2}$$

Two docking dynamics frequencies ω_1 and ω_2 are:

$$\begin{cases} \omega_1 = \sqrt{\dfrac{\frac{k_m}{m_e} + \frac{k_p}{m} - \sqrt{\left(\frac{k_m}{m_e} + \frac{k_p}{m}\right)^2 - \frac{4k_m k_p}{m_s m_e}}}{2}} \\ \omega_2 = \sqrt{\dfrac{\frac{k_m}{m_e} + \frac{k_p}{m} + \sqrt{\left(\frac{k_m}{m_e} + \frac{k_p}{m}\right)^2 - \frac{4k_m k_p}{m_s m_e}}}{2}} \end{cases} \tag{3}$$

where $m = \frac{m_e m_s}{m_s + m_e}$.

B. FORCE MEASUREMENT MODEL

The force measurement system includes a force sensor, an amplifier and a data acquisition card. There is a time delay from the actual force $f_{act}(t)$ to the measured force $f_{mea}(t)$. The delay caused by the force sensor and its amplifier can be approximated to a first-order model with a delay time of T_f, which is as follows:

$$F(s) = 1/\left(1 + T_f s\right) \tag{4}$$

C. CONTACT MODEL

The actual force $f_{act}(t)$ can be obtained by the actual displacement of the motion simulator s_{act}, the velocity of the drag mechanism v and five attribute parameters; the derivation process is given as follows. Set the displacement and velocity of the end-effector are x_e and $\dot{x}_e$; the relative displacement and velocity of the drag mechanism and the end-effector in the body coordinate system of the end-effector are x (x is equal to zero at the initial time of the drag) and $v(v = \dot{x})$; then, the displacement of the drag mechanism x_d in the inertial coordinate O_e is:

$$x_d = x_e + x \tag{5}$$

Laplace transformation of Eq. 5:

$$X_d = X_e + X; X = \frac{V}{s} \tag{6}$$

Equilibrium equation of the end-effector is:

$$m_e \ddot{x}_e = -k_m x_e - c_m \dot{x}_e + k_p\left(s_{act} - x_d\right) + c_p\left(\dot{s}_{act} - \dot{x}_d\right) \tag{7}$$

Laplace transformation of Eq. 7:

$$m_e X_e s^2 = -k_m X_e - c_m X_e s + k_p\left(S_{act} - X_d\right) + c_p\left(S_{act} - X_d\right) s \tag{8}$$

The actual force $f_{act}(t)$ is:

$$f_{act}(t) = -k_m x_e - c_m \dot{x}_e \tag{9}$$

Laplace transformation of Eq. 9:

$$F_{act} = -k_m X_e - c_m X_e s \tag{10}$$

According to Eq. 6, Eq. 8 and Eq. 10, the Laplace transformation of the actual force $f_{act}(t)$ is obtained as follows:

$$F_{act} = \frac{\left(k_m + c_m s\right)\left(k_p + c_p s\right)}{m_s s^2 + \left(c_m + c_p\right) s + k_m + k_p}\left(S_{act} - X\right) \tag{11}$$

The actual force of the motion simulator under the displacement of s_{act} is obtained in Eq. 11. Then, the desired force model with respect to the desired displacement s_{des} can be obtained based on the above deduction:

$$F_{des} = \frac{\left(k_m + c_m s\right)\left(k_p + c_p s\right)}{m_s s^2 + \left(c_m + c_p\right) s + k_m + k_p}\left(S_{des} - X\right) \tag{12}$$

The deviation between the actual force corresponding to the actual position and the desired force corresponding to the desired position can be obtained by the Eq. 11 and Eq.12:

$$\begin{aligned} \Delta F_{dev} &= F_{des} - F_{act} \\ &= \frac{\left(k_m + c_m s\right)\left(k_p + c_p s\right)}{m_s s^2 + \left(c_m + c_p\right) s + k_m + k_p}\left(S_{des} - S_{act}\right) \end{aligned} \tag{13}$$

According to Eq. 13, the deviation of the force is only related to the five attribute parameters, the desired displacement of the motion simulator and the actual displacement of the motion simulator; which is independent of the motion state of the drag mechanism and the dynamics response delay model of the motion simulator.

D. MOTION SIMULATOR MODEL

A multi-rigid-body dynamics model and a control model of the motion simulator, as shown in Fig. 8, are established to analyze the displacement phase characteristics of motion simulator in the dynamics frequency range, so as to establish the phase lead compensation model.

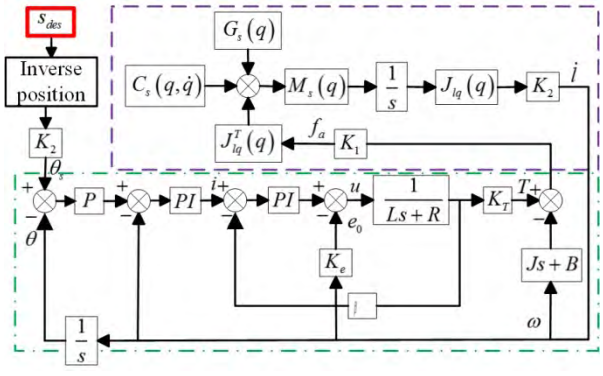

FIGURE 8. A multi-rigid-body dynamics model and a control model of the motion simulator.

The dotted line region is a multi-rigid-body dynamics model of the motion simulator based on the Kane's method;

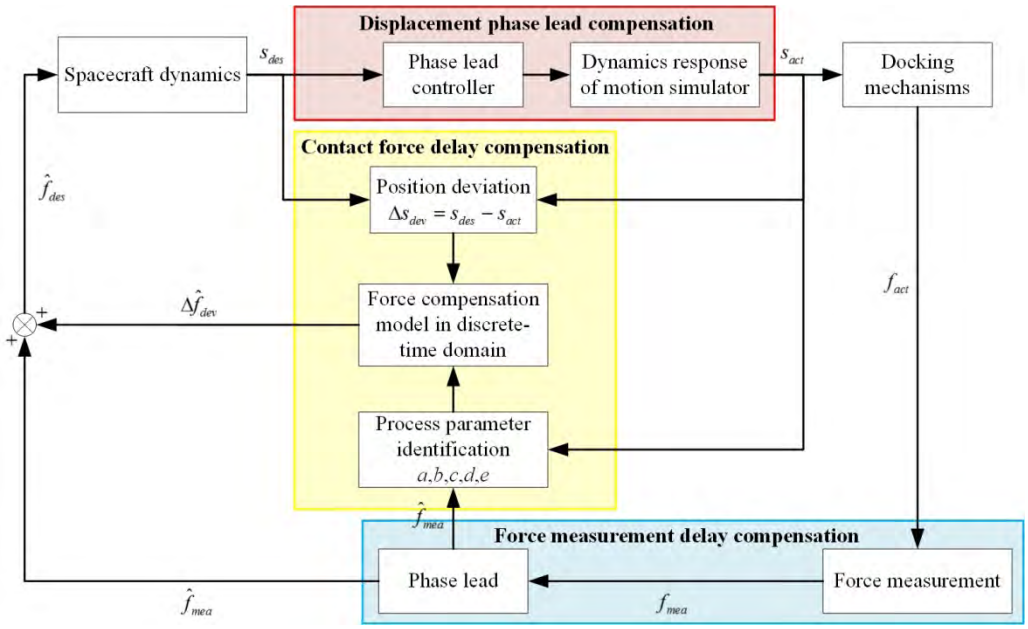

FIGURE 9. Principle of the force and displacement compensation method.

where q is the six-DOF attitude of the motion simulator; $M_s(q)$ denotes the mass matrix of the motion simulator's platform and leg in the inertial coordinate system; $C_s(q, \dot{q})$ is the Coriolis term in the inertial system; $G_s(q)$ is the gravity and the external force in the inertial coordinate system; $J_{lq}(q)$ is the velocity Jacobian matrix. The dash-dot line region is the control system model of the motor; where PI denotes the proportional-integral controller; P denotes the proportional controller; L and R are the inductance and resistance of the motor, respectively; K_e is the back EMF coefficient of the motor; K_T is the torque coefficient; J and B are the equivalent inertia and damping of electric cylinder and motor, respectively; K_2 is the velocity conversion coefficient of the electric cylinder and the motor; K_1 is the reciprocal of K_2; β is a current feedback coefficient; f_a and $\dot{l}$ are the output force and line velocity of electric cylinders. The six electric cylinders of the motion simulator have the same characteristics, so are the six motors; and the diagram of the control principle for one motor is shown in Fig. 8.

IV. COMPENSATION METHOD TOWARDS THE HIL SIMULATION FOR MANIPULATOR DOCKING

A force and displacement compensation method is proposed, as shown in Fig. 9, to prevent the simulation divergence and improve the accuracy of reproduction. If the compensated force $\hat{f}_{des}$ is equal to the force f_{des} corresponding to the desired position, then, the desired position at the next moment of the spacecraft can be obtained through the dynamics model. If the compensated position of the motion simulator s_{act} is equal to the desired position s_{des}, then, the motion simulator can accurately reproduce the docking process.

A. FORCE MEASUREMENT DELAY COMPENSATION

The time lead $1+T_f s$ can fully compensate the time delay $1/(1+T_f s)$ of Eq. 4. Therefore, the compensation model of the force measurement delay is given by:

$$C_{comp}(s) = 1 + T_f s \tag{14}$$

B. CONTACT FORCE DELAY COMPENSATION

1) DISCRETIZATION OF CONTACT FORCE MODEL AND FORCE COMPENSATION MODEL

When identifying parameters, the continuous-time contact force model is discretized to get the difference equation. The differential transformation, zero-order hold and bilinear transformation are the commonly used discrete methods. The following difference equation of Eq. 11 can be obtained in any discrete method:

$$\begin{aligned}\hat{f}_{act}(k) = {} & a\hat{f}_{act}(k-1) + b\hat{f}_{act}(k-2) \\ & + c\,(s_{act}(k) - x(k)) + d\,(s_{act}(k-1) - x(k-1)) \\ & + e\,(s_{act}(k-2) - x(k-2)), \quad k = 2, 3, \cdots\end{aligned} \tag{15}$$

where $\hat{f}_{act}(k)$, $\hat{f}_{act}(k-1)$ and $\hat{f}_{act}(k-2)$ are the forces after the contact force delay compensation, $s_{act}(k)$, $s_{act}(k-1)$ and $s_{act}(k-2)$ are the displacements of the motion simulator, $x(k)$, $x(k-1)$ and $x(k-2)$ are the relative displacements of the drag mechanism and the end-effector; which are stored in real-time and are known parameters. a, b, c, d, e are the process parameters that need to be identified. By different discrete methods, theoretical values of the process parameters are different; the backward difference method is used in this

study, the theoretical values are as follows:

$$\begin{cases} a_t = \dfrac{2m_e + (c_m + c_p)T}{m_e + (c_m + c_p)T + (k_m + k_p)T^2} \\ b_t = -\dfrac{m_e}{m_e + (c_m + c_p)T + (k_m + k_p)T^2} \\ c_t = \dfrac{c_m c_p + (c_m k_p + c_p k_m)T + k_m k_p T^2}{m_e + (c_m + c_p)T + (k_m + k_p)T^2} \\ d_t = -\dfrac{2c_m c_p + (c_m k_p + c_p k_m)T}{m_e + (c_m + c_p)T + (k_m + k_p)T^2} \\ e_t = \dfrac{c_m c_p}{m_e + (c_m + c_p)T + (k_m + k_p)T^2} \end{cases} \tag{16}$$

The difference equation of the compensation force is obtained by discretizing the force compensation model of Eq. 13:

$$\begin{aligned} \Delta\hat{f}_{dev}(k) = {} & a\Delta\hat{f}_{dev}(k-1) + b\Delta\hat{f}_{dev}(k-2) \\ & + c\Delta s_{dev}(k) + d\Delta s_{dev}(k-1) + e\Delta s_{dev}(k-2) \end{aligned} \tag{17}$$

where $\Delta\hat{f}_{act}(k-1)$ and $\Delta\hat{f}_{act}(k-2)$ are the compensation forces, $\Delta s_{dev}(k)$, $\Delta s_{dev}(k-2)$ and $\Delta s_{dev}(k-2)$ are the displacement deviations of the motion simulator; which are stored in real-time and are known parameters; therefore, the compensation force $\Delta\hat{f}_{act}(k)$ can be obtained by combining the identification results of the process parameters. If the sampling time for discrete points is equal to the time interval of the system simulation, the desired force $\hat{f}_{des}$at any moment can be obtained:

$$\hat{f}_{des}(t) = \hat{f}_{mea}(t) + \Delta\hat{f}_{dev}(t) \tag{18}$$

2) REAL-TIME PARAMETER IDENTIFICATION BASED ON KALMAN-FILTER

The identification results will be affected by the noise interference of the force sensor and the accidental friction of the mechanisms during the docking process; especially when the number of the identification objects is large. Thus, Kalman-filter identification method is used in this study for its strong anti-noise interference and good stability; in addition, this identification method has high accuracy for the system with large variation in parameters. We assume the linear system of Eq. 15 can be described as:

$$\begin{cases} Y(k+1) = \Phi(k+1,k)\,Y(k+1) + \Gamma(k+1,k)W(k) \\ Z(k) = H(k)\,Y(k) + V(k) \end{cases} \tag{19}$$

where $W(k)$ is the friction noise and sensor measurement noise, $V(k)$ is the system process noise, and:

$$\begin{cases} \Gamma = \Phi = I \\ Z(k) = \hat{f}_{act}(k) \\ H(k) = \left[\hat{f}_{act}(k-1)\ \hat{f}_{act}(k-2)\ s_{act}(k) - x(k)\right. \\ \quad \left. s_{act}(k-1) - x(k-1)\ s_{act}(k-2) - x(k-2)\right] \\ Y(k) = \left[a(k)\ b(k)\ c(k)\ d(k)\ e(k)\right]^T \end{cases} \tag{20}$$

The Kalman-filter identification model is as follows:

$$\begin{cases} \hat{Y}(k|k) = \hat{Y}(k-1|k-1) \\ \quad + K(k)\left[Z(k) - H(k)\,\hat{Y}(k-1|k-1)\right] \\ K(k) = \dfrac{P(k|k-1)\,H^T(k)}{\left[H(k)\,P(k|k-1)\,H^T(k) + R_k\right]} \\ P(k|k-1) = P(k|k-1) + Q_{k-1} \\ P(k|k) = [I - K(k)\,H(k)]\,P(k|k-1) \end{cases} \tag{21}$$

where Q_{k-1} and R_k are the covariance matrixes of $V(k)$ and $W(k)$, respectively; $P(k|k)$ is the error covariance matrix; $K(k)$ is the Kalman-gain; $Y(k|k) = [a(k)\ b(k)\ c(k)\ d(k)\ e(k)]$.

The initial values $Y(0|0)$ and $P(0|0)$ need to be set before the identification. In order to get the accurate identification results quickly, we can estimate the five attribute parameters to calculate the approximate ranges of the process parameters; and the initial values $Y(0|0)$ and $P(0|0)$ are taken in this range.

C. DISPLACEMENT PHASE DELAY COMPENSATION

By estimating the approximate ranges of the five attribute parameters, dynamics frequency ranges can be obtained based on Eq. 3. It is found that the amplitude of the high frequency oscillation is very small, and it quickly attenuates to disappear under the effect of damping. The docking process is fundamental frequency motion (low frequency motion), thus, the displacement phase lead compensation model of the motion simulator can be established according to the low frequency range. The range of the phase angle $\varphi(\varphi \in [\varphi_{\min}\ \varphi_{\max}])$ within the range of the dynamics frequency $\omega_1(\omega_1 \in [\omega_{\min}\ \omega\ _{\max}])$ is obtained by the motion simulator model of Fig. 8. The displacement phase lead compensation model is:

$$G_{comp}(s) = K\frac{1+\alpha Ts}{1+Ts} \tag{22}$$

The maximum positive phase angle $\psi_{\max}$ that the compensation model of Eq. 22 can provide and the corresponding frequency ω_m are expressed as:

$$\psi_{\max} = \sin^{-1}\frac{\alpha-1}{\alpha+1}; \quad \omega_m = 1/\left(\sqrt{\alpha}T\right) \tag{23}$$

The delay phase angle of the motion simulator increases with the increase of the frequency; therefore, the maximum phase angle $\varphi_{\max}$ is got at frequency of $\omega_{\max}$, set:

$$\psi_{\max} = \varphi_{\max} = \sin^{-1}\frac{\alpha-1}{\alpha+1}; \quad \omega_m = \omega_{\max} = 1/\left(\sqrt{\alpha}T\right) \tag{24}$$

Then α and T in the compensation model can be obtained. K is calculated according to the amplitude deviation generated by $(1+\alpha Ts)/(1+Ts)$ at the frequency of ω_m. Although the proposed displacement phase lead compensation model can reduce the phase delay of the motion simulator in the dynamics frequency range, the delay of the HIL simulation system cannot be completely eliminated by only using this compensation model, and the HIL simulation system still has

the divergence and the loss of accuracy. The displacement phase lead compensation method should be used with the force compensation method.

V. VERIFICATIONS

A. SIMULATION VERIFICATIONS

The HIL simulation system model for space manipulator, as shown in Fig. 9, was established using the Simulink module of the Matlab software. The drag mechanism moves at a constant speed, thus, the displacement curve of the motion simulator is close to an oblique line; however, it is difficult to observe the frequency characteristics and the reproduction accuracy under the gradual curves. The oscillation curves are convenient to compare the performances of different compensation methods. So set the drag mechanism was stationary in the simulation and experiment, respectively; and the motion simulator offset downward 10 mm and 5 mm from the equilibrium position (contact force was zero), respectively, which made the wire rope and the spring mechanism deform; then the HIL simulation system came into the dynamics stage, the push and pull oscillation process of the spacecraft under the contact force was simulated. Because there was no precise measurement delay model of the force sensor, it was considered that the force sensor had no delay in the simulation, only had the friction noise and force measurement noise $n(t)$ (and $R_k(n)$=0.001); then the variables relationship of the 'force measurement delay compensation' in Fig. 9 was:

$$\begin{cases} f_{mea}(t) = f_{act}(t) \\ \hat{f}_{mea}(t) = f_{mea}(t) + n(t) \end{cases} \tag{25}$$

The validity of the contact force delay compensation (CFDC) and the displacement phase delay compensation (DPDC) were verified by simulation. The validity of the force measurement delay compensation (FMDC) was only verified by experiments.

1) THE EFFECTIVENESS OF THE COMPENSATION METHOD

The simulation parameters are selected based on the range of the physical parameters in the real space docking. Because of the flexibility of the space manipulator, the docking dynamics frequency (fundamental frequency) is usually within 2 Hz; firstly a set of the parameters in the lower dynamics frequency range is selected as shown in Table 1.

The displacements of the motion simulator with different compensation methods are shown in Fig. 10. The ideal curve in the Fig. 10 refers to the motion displacement of the spacecraft in the real space docking, and the dynamics frequency is 0.97 Hz. We can get that the displacement of the motion simulator is divergent without the compensation method; the CFDC compensation method can prevent the divergence of the system. Due to the displacement phase delay of the motion simulator, there are phase deviation and accuracy loss in the displacement with the CFDC method; which are small when the motion frequency is small. The displacement with the CFDC+DPDC method basically coincides with the ideal displacement. It can be seen that the DPDC method improves the reproduction accuracy of the HIL simulation system.

TABLE 1. Low-frequency simulation parameters.

Parameters	Value
Mass of spacecraft m_s (kg)	1000
Mass of end-effector m_e (kg)	150
Stiffness of manipulator k_m (N/m)	1.5e5
Damping of manipulator c_m (N/(m/s))	200
Contact stiffness k_p (N/m)	5e4
Contact damping c_p (N/(m/s))	100
Discrete time T (s)	0.001

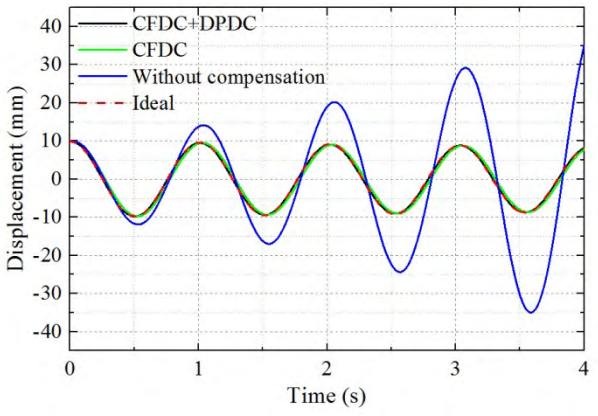

FIGURE 10. Displacements of the motion simulator with different compensation methods (at dynamics frequency of 0.97 Hz).

Set the initial values Y(0|0)= [135 −428 350 −1.1 2.1]. The identification results of process parameters with noise are shown in Fig. 11, which indicate the Kalman-filter identification method can obtain accurate results in the case of noise. Five attribute parameters can be calculated by Eq. 16, as shown in Fig. 12.

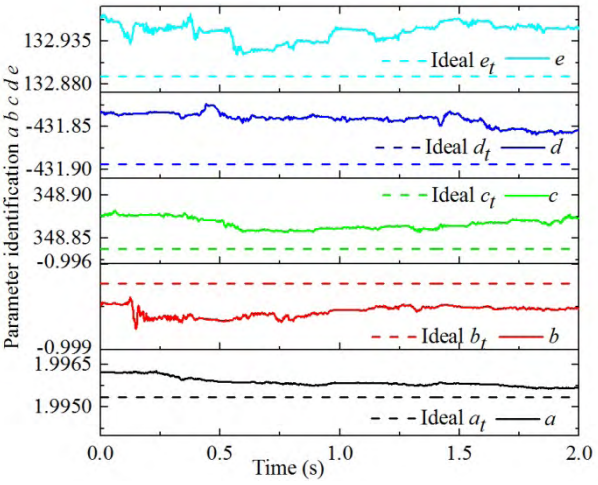

FIGURE 11. Identification results of the process parameters.

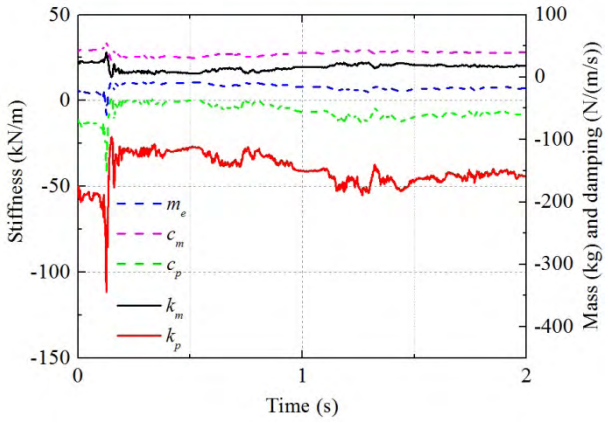

FIGURE 12. Calculation of the attribute parameters.

Because there is a small deviation of process parameters between the identification results and the theoretical values, the attribute parameters calculated by Eq. 16 are singular. The attribute parameters are seriously distorted, and some parameters have negative values. Therefore, the continuous-time domain model cannot be used for compensation.

The ideal force, the measured force without compensation and the compensated force with CFDC method are given in Fig. 13. It shows that the measured force without compensation is delayed to the ideal force, while the phase of the compensated force is close to the ideal one. The phase delay between the measured force and the ideal one is compensated; therefore the simulation is no longer divergent.

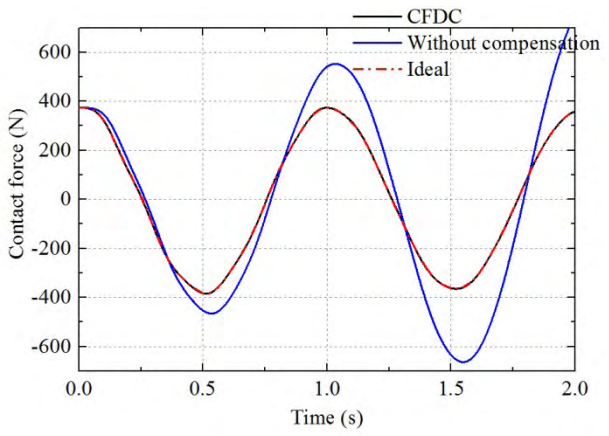

FIGURE 13. Contact forces under different conditions (at dynamics frequency of 0.97 Hz).

2) THE EFFECTIVENESS OF CFDC+DPDC WITH DIFFERENT DIFFERENCE METHODS

The difference equation of the Eq. 15 can be obtained through three difference methods including the forward difference, the backward difference and the bilinear transformation, but the theoretical values of the process parameters are different under three difference methods. By selecting different identification initial values, the identification results of the process parameters under the three difference methods can be obtained; and the corresponding displacements of the motion simulator with the CFDC+DPDC method are shown in Fig. 14. Although the identification results of process parameters are different, they all prevent the system from diverging and have high reproduction accuracy; which reflect the flexibility of the discrete-time domain compensation model.

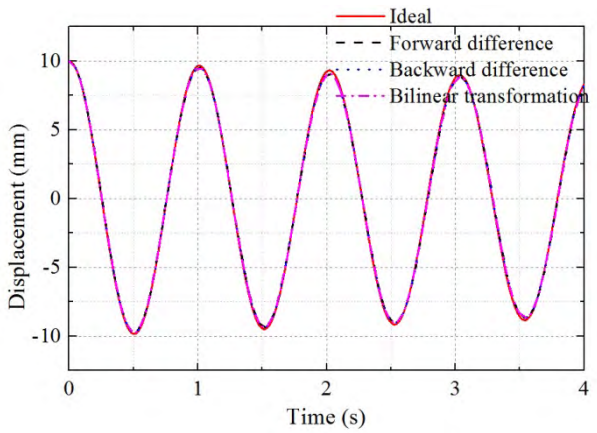

FIGURE 14. The displacements with CFDC+DPDC compensation method under three difference methods (at dynamics frequency of 0.97 Hz).

3) THE EFFECTIVENESS OF THE COMPENSATION METHOD FOR TIME-VARYING PARAMETERS

A set of parameters in the range of high dynamics frequency, as shown in Table 2, is selected to study the effectiveness of the compensation model for the constant parameter system and the time-varying parameter system.

TABLE 2. High-frequency simulation parameters.

Parameters	Value
Mass of spacecraft m_s (kg)	500
Mass of end-effector m_e (kg)	100
Stiffness of manipulator k_m (N/m)	5.6e5
Damping of manipulator c_m (N/(m/s))	400
Contact stiffness k_p (N/m)	1.6e5
Contact damping c_p (N/(m/s))	400
Discrete time T (s)	0.001

The displacements of the motion simulator with different compensation methods are shown in Fig. 15. The dynamics frequency is 2.6 Hz. With the increase of the dynamics frequency, the system divergence is faster and more obvious without compensation. The application of CFDC method can prevent the system from diverging, but the delay and attenuation of the motion simulator's displacement are obvious at high frequency, and the loss of accuracy is great. The CFDC+DPDC method can obtain the ideal reproduction result.

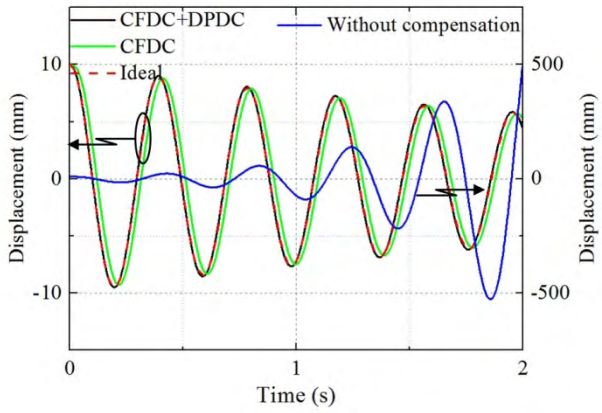

FIGURE 15. Displacements of the motion simulator with different compensation methods (at dynamics frequency of 2.6 Hz).

The ideal force, measured force without compensation and the compensated force with the CFDC method are given in Fig. 16. Compared with the ideal force, the measured force without compensation has a large delay and a rapid divergence. The phase of the compensated force with the CFDC method is close to the ideal force.

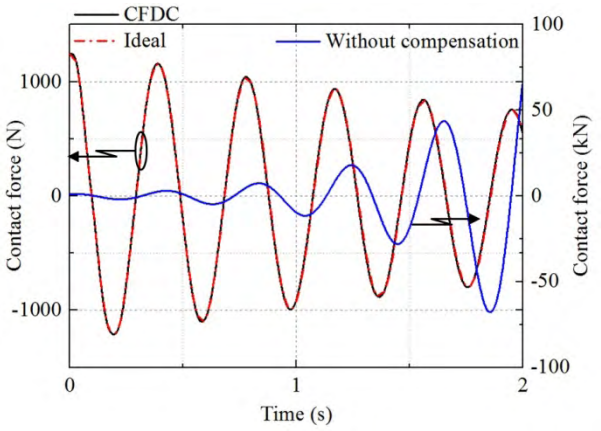

FIGURE 16. Contact forces under different conditions (at dynamics frequency of 2.6 Hz).

A sine signal with amplitude of 8e4 N/m and frequency of 1 Hz is superposed with the contact stiffness k_p in Table 2 to simulate the time-varying parameter. The CFDC+DPDC compensation method is used in the time-varying parameter system, the corresponding displacement of the motion simulator is shown in Fig. 17; which indicates that the CFDC+DPDC method can prevent the divergence of the time-varying systems and ensure the system with high reproduction accuracy. The changes of k_p have a great impact on the process parameters of c and d, and the identification results are shown in Fig. 18. We can obtain that Kalman-filter method for identifying of the time-varying parameters is still accurate.

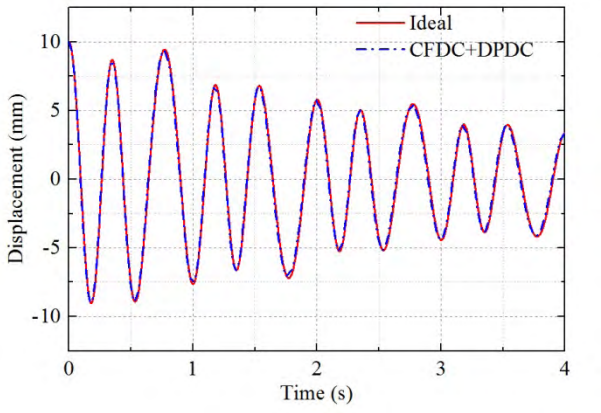

FIGURE 17. The displacements of the time-varying system with the CFDC+DPDC method.

Results of the identification and the force compensation are also obtained by using the recursive least square (RLS) method, the corresponding displacement and identification parameters of the motion simulator are shown in Fig. 19 and Fig. 20, respectively. Using the RLS identification method, the identification accuracy of the

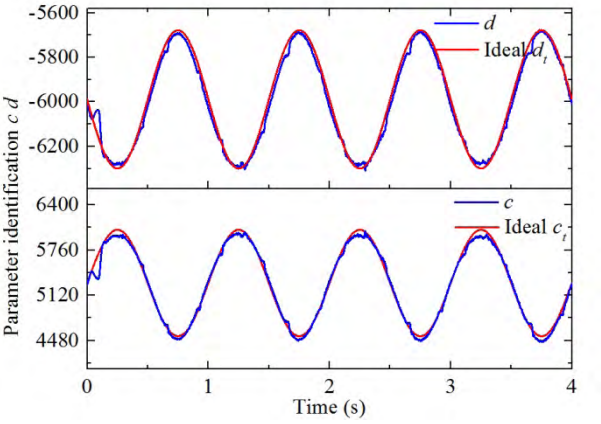

FIGURE 18. Identification results of the process parameters c and d.

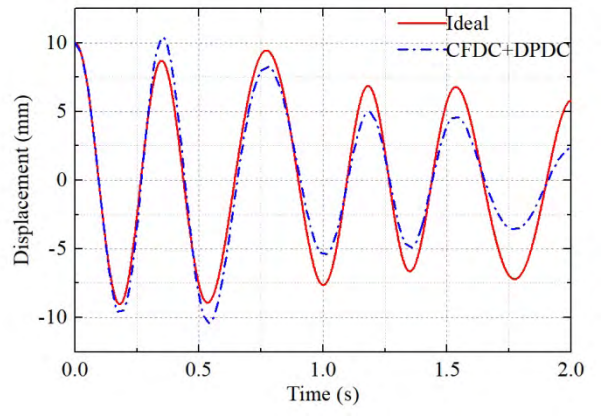

FIGURE 19. The displacements of the time-varying system with the CFDC+DPDC method using the RLS method.

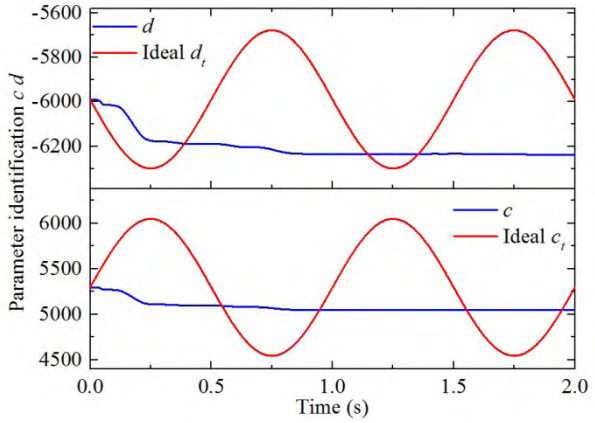

FIGURE 20. Identification results of the process parameters *c* and *d* using the RLS method.

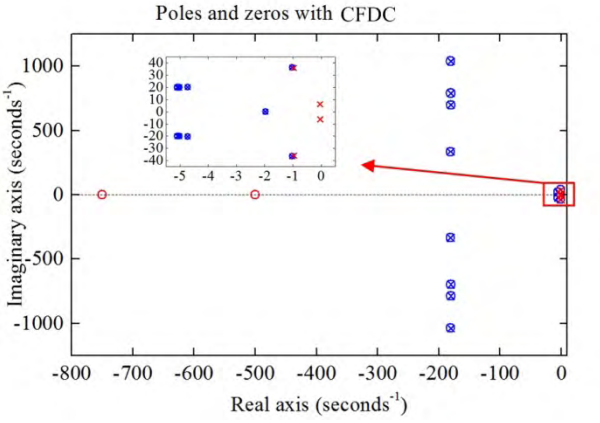

FIGURE 22. Poles and zeros of the closed-loop HIL simulation system with CFDC compensation method.

time-varying parameters and the effect of force compensation are poor. The Kalman-filter identification method can improve the recognition response by adjusting the covariance Q_{k-1} of the process noise.

4) POLES ANALYSIS OF THE CLOSED-LOOP SYSTEM BASED ON COMPENSATION METHOD

To further explain how the force compensation method can prevent the system from diverging, the poles analysis method is utilized to analyze the closed-loop characteristics of the HIL simulation system. The ideal system model (real space docking in Fig. 4) and the actual system model (in Fig. 5) with CFDC compensation method are established by the Simulink, and the poles and zeros of the two systems are further obtained through the 'New Pole/Zero Map' tool in the Simulink, which are shown in Fig. 21 and Fig. 22, respectively. The poles are plotted as 'x' and the zeros are plotted as 'o'. Some poles and zeros of the closed-loop HIL simulation system are canceled with the CFDC compensation method, and the remaining ones are close to those of the ideal system. That is why the compensated HIL simulation system can approximate the ideal system.

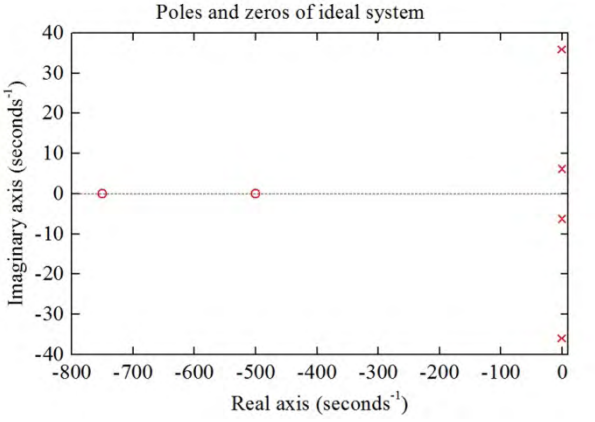

FIGURE 21. Poles and zeros of the ideal closed-loop system.

B. EXPERIMENTAL VERIFICATIONS

The experimental facilities of the HIL simulation system for manipulator docking were shown in Fig. 23. Due to the classified reasons, pictures of the end-effector and the target-adapter can't be provided, and pictures of the other main structures were presented separately. A spring with known stiffness and damping (the stiffness of the spring was within the stiffness range of the wire rope) was used to simulate the elastic of the wire rope. Dynamics calculation of the spacecraft and control of the motion simulator were accomplished by two sets of upper and lower computers. The upper and lower computers transmitted data through Ethernet, and two lower computers transmitted data through reflective memory. In the experiment, the Xpc real-time simulation system of MATLAB was applied, and the sampling period was

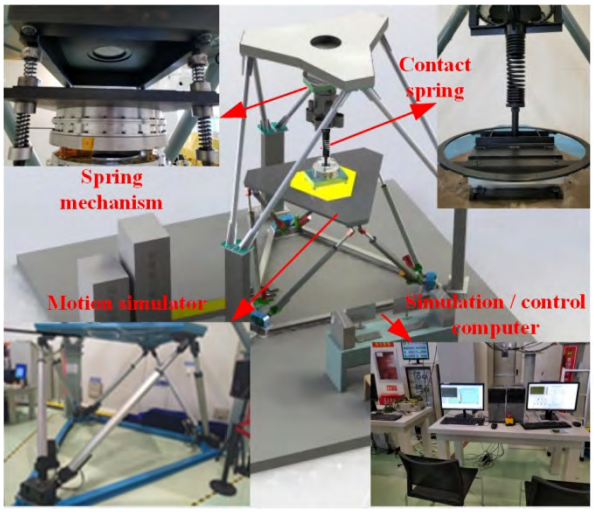

FIGURE 23. The experimental facilities of the HIL simulation system.

set as 1 ms. The initial displacement offset of the motion simulator was 5 mm in vertical direction, and the contact force was measured by the force sensor (FP4060-10-2000, BERTEC, American), then the HIL simulation system came into the dynamics calculation process.

The experimental parameters are listed in Table 3, and the dynamics frequency is 0.43 Hz. The displacements of the motion simulator with different compensation methods are shown in Fig. 24. It can be seen that the displacement of the motion simulator is divergent without compensation method; the separate use of FMDC method and CFDC method only slows the divergence trend, but doesn't prevent the divergence; CFDC+FMDC compensation method can prevent the system from diverging, and due to the displacement phase delay of the motion simulator, the reproduction accuracy is slightly lost; the displacement with the CFDC+FMDC+DPDC compensation method coincides with the ideal displacement.

TABLE 3. The experimental parameters.

Parameters	Value
Mass of spacecraft m_s (kg)	5000
Mass of end-effector m_e (kg)	136
Stiffness of manipulator k_m (N/m)	1.45e5
Damping of manipulator c_m (N/(m/s))	150
Contact stiffness k_p (N/m)	4.97e4
Contact damping c_p (N/(m/s))	120
Discrete time T (s)	0.001
Force measurement delay T_f (ms)	9

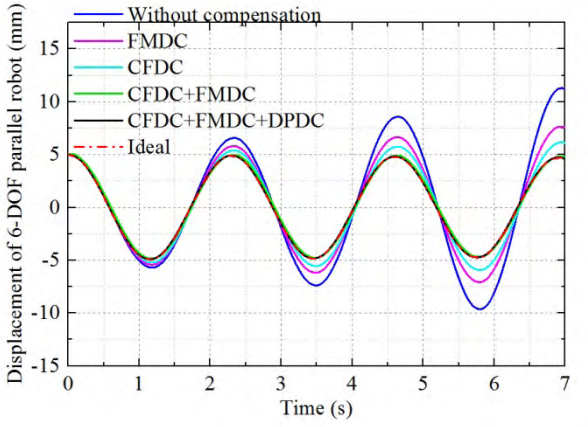

FIGURE 24. Displacements of the motion simulator with different compensation methods in experiment (at dynamics frequency of 0.43 Hz).

The theoretical values of the process parameters are approximately: a=1.95; b=−1.01; c=370.42; d=−450.02; e=131.95. The identification results of the process parameter are shown in Fig. 25, which show Kalman-filter identification method has high accuracy. The ideal force, the compensated force with FMDC method and the compensated force with CFDC+FMDC method are given in Fig. 26. And the

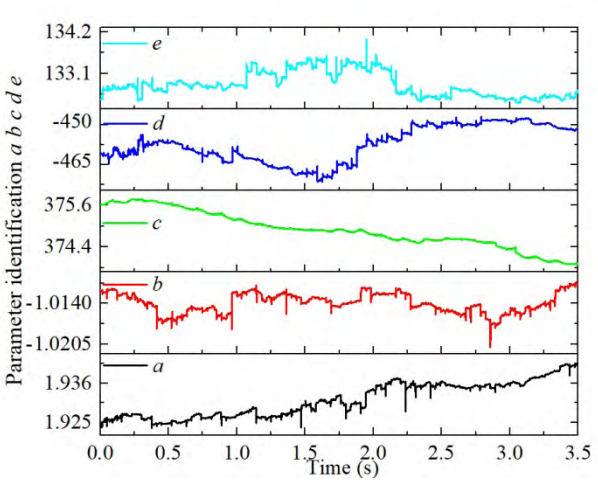

FIGURE 25. Identification results of the process parameters in experiment.

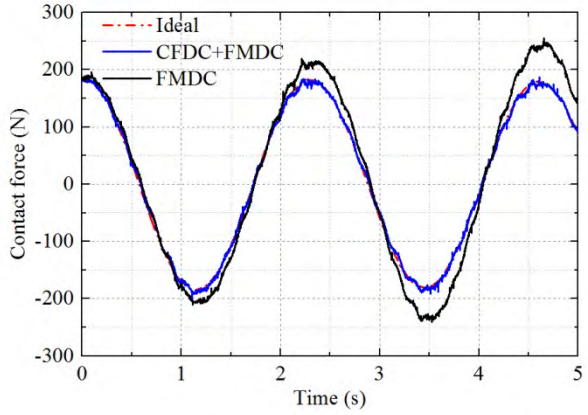

FIGURE 26. Contact forces under different conditions in experiment (at dynamics frequency of 0.43 Hz).

measurement force has a phase delay by only using the FMDC compensation method. The phase of the compensated force with the CFDC+FMDC approximates the phase of the ideal force.

The mass of the spacecraft is set to 1000 kg to simulate high dynamics frequency, and the corresponding dynamics frequency is 0.87 Hz. The displacements of the motion simulator with different compensation methods are shown in Fig. 27. With the increase of the dynamics frequency, the system divergence is faster and more obvious without compensation; the CFDC+FMDC method can prevent the divergence of the system; after adding the DPDC method, the reproduction result approximate the ideal result. The ideal force, the compensated force with FMDC method and the compensated force with CFDC+FMDC method are shown in Fig. 28. The phase of the compensated force with the CFDC+FMDC method is close to that of the ideal force.

From the above experiments, we can obtain that simulation divergence problem of the HIL simulation system for space

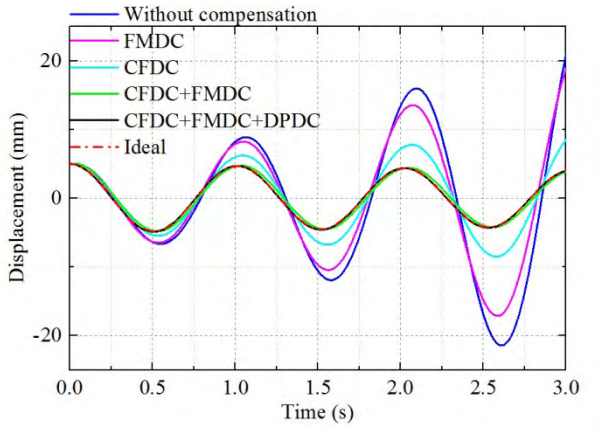

FIGURE 27. Displacements of the motion simulator with different compensation methods in experiment (at dynamics frequency of 0.87 Hz).

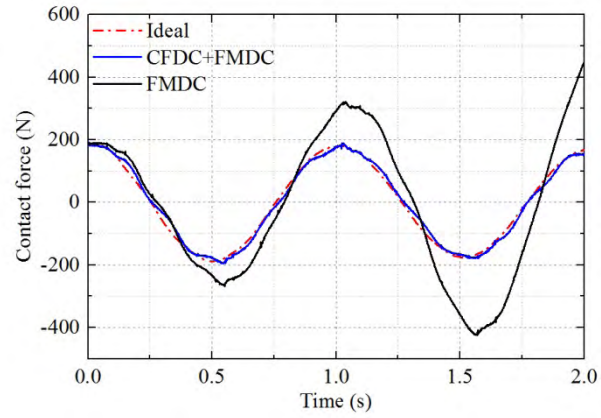

FIGURE 28. Contact forces under different conditions in experiment (at dynamics frequency of 0.87 Hz).

manipulator docking is prevented by using the proposed force compensation method and the reproduction accuracy is further improved by using the displacement phase compensation method. Then, the satisfactory simulation fidelity is achieved.

VI. CONCLUSIONS

The divergence and accuracy problem of the manipulator docking HIL simulation for the multi-stiffness, multi-damping and single-mass contact was solved by a force and displacement compensation method. The force compensation included the force measurement delay compensation and the contact force delay compensation. The phase lead based force compensation was effective to compensate the force measurement delay. A discrete force compensation model based on real-time identification parameters was used to compensate the contact force delay. In the condition of noise interference and time-varying parameters, accurate results of the identification parameters can be obtained by applying of the Kalman-filter identification method. And the discrete-time domain compensation model avoided the parameter singularity of the continuous-time domain model, which obtained the accurate compensation force. In addition, the force compensation was the model-free compensation. The displacement phase lead compensation model based on the dynamics frequency was effective to reduce the displacement phase delay of the motion simulator, which improved the reproduction accuracy of the HIL simulation system. Simulations and experiments verified that the satisfactory simulation fidelity can be achieved by the proposed force and displacement compensation method. In the future, the proposed method will be extended to a six-DOF space contact.

REFERENCES

[1] K. Zhang, H. Zhou, Q. Wen, and R. Sang, "Review of the development of robotic manipulator for international space station," *Chin. J. Space Sci.*, vol. 30, no. 6, pp. 612–619, 2010.

[2] W.-H. Zhang, X-P. Ye, X.-M. Ji, X.-L. Wu, Y.-F. Zhu, and C. Wang, "Development summarizing of space robot technology national and outside," (in Chinese), *Flight Dyn.*, vol. 31, pp. 198–202, Mar. 2013, doi: 10.13645/j.cnki.f.d.2013.03.001.

[3] F. Feng, Y. Liu, H. Liu, and H. Cai, "Design schemes and comparison research of the end-effector of large space manipulator," *Chin. J. Mech. Eng.*, vol. 25, no. 4, pp. 674–687, 2012.

[4] W. Xu, B. Liang, and Y. Xu, "Survey of modeling, planning, and ground verification of space robotic systems," *Acta Astron.*, vol. 68, pp. 1629–1649, Jun./Jul. 2011.

[5] A. Flores-Abad, O. Ma, K. Pham, and S. Ulrich, "A review of space robotics technologies for on-orbit servicing," *Prog. Aerosp. Sci.*, vol. 68, pp. 1–26, Jul. 2014.

[6] D. Zeng, Y. Yang, D. Cong, and C. Yang, "Space end effector capturing hybrid simulation system," in *Proc. Int. Conf. Fluid Power Mechatronics (FPM)*, 2015, pp. 448–453.

[7] H. Zhao and S. Zhang, "Stability research of space docking dynamics simulation based on Stewart platform," *Mach. Tool Hydraul.*, vol. 8, pp. 48–50, Aug. 2006.

[8] H. Zhao and S. Y. Zhang, "Stability analysis of the whole dynamics simulation system of space docking," (In Chinese), *J. Wuhan Univ. Sci. Tech. (Natural Sci. Ed.)*, vol. 31, no. 1, pp. 87–90, Feb. 2008, doi: 10.3969/j.issn.1674-3644.2008.01.020.

[9] F. Feng, "Research on space large misalignment tolerance end-effector and its soft capture strategy," Ph.D. dissertation, Dept. Mech. Eng., Harbin Inst. Technol., Harbin, China, 2013.

[10] S. Yu, Z. Qu, S. Zheng, and J. Han, "Capture dynamics modeling and simulation of the space flexible manipulator," in *Theory, Methodology, Tools and Applications for Modeling and Simulation of Complex Systems*. Singapore: Springer, 2016, pp. 296–307

[11] D. R. Riley, B. M. Jaquet, J. E. Pennington, and R. F. Brissenden, "Comparison of results of two simulations employing full-size visual cues for pilot-controlled Gemini-Agena docking," NASA, Washington, DC, USA, Tech. Note TN D-3687, Nov. 1967, pp. 1–35.

[12] H. G. Hatch, Jr., J. E. Pennington, and J. B. Cobb, "Dynamic simulation of lunar module docking with Apollo command module in lunar orbit," NASA, Washington, DC, USA, Tech. Note TN D-3972, Jun. 1967, pp. 1–26.

[13] O. Ma, A. Flores-Abad, and T. Boge, "Use of industrial robots for hardware-in-the-loop simulation of satellite rendezvous and docking," *Acta Astron.*, vol. 81, no. 1, pp. 335–347, Aug. 2012.

[14] T. Chang, D. Cong, Z. Ye, and J. Han, "Time problems in HIL simulation for on-orbit docking and compensation," in *Proc. 2nd IEEE Conf. Ind. Electron. Appl.*, May 2007, pp. 841–846.

[15] H. Shimoji, M. Inoue, K. Tsuchiya, K. Niomiya, and I. K. J. Nakatani, "Simulation system for a space robot using six-axis servos," *Adv. Robot.*, vol. 6, no. 2, pp. 179–196, Jan. 1991.

[16] K. Osaki, A. Konno, and M. Uchiyama, "Delay time compensation for a hybrid simulator," *Adv. Robot.*, vol. 24, nos. 8–9, pp. 1081–1098, Apr. 2010.

[17] S. Abiko, Y. Satake, X. Jiang, T. Tsujita, and M. Uchiyama, "Delay time compensation based on coefficient of restitution for collision hybrid motion simulator," *Adv. Robot.*, vol. 28, no. 17, pp. 1177–1188, Sep. 2014.

[18] S. Ananthakrishnan, R. Teders, and K. Alder, "Role of estimation in real-time contact dynamics enhancement of space station engineering facility," *IEEE Robot. Autom. Mag.*, vol. 3, no. 3, pp. 20–28, Sep. 1996.

[19] M. Zebenay, T. Boge, R. Krenn, and D. Choukroun, "Analytical and experimental stability investigation of a hardware-in-the-loop satellite docking simulator," *Proc. Inst. Mech. Eng. G, J. Aerosp. Eng.*, vol. 229, no. 4, pp. 666–681, Mar. 2015.
[20] C. Qi, X. Zhao, F. Gao, A. Ren, and Y. Hu, "Divergence compensation for hardware-in-the-loop simulation of stiffness-varying discrete contact in space," *Acta Astronaut.*, vol. 128, pp. 295–303, Nov./Dec. 2016.

SIMIAO YU was born in Mudanjiang, Heilongjiang, China, in 1988. He received the B.S. degree from the College of Mechanical and Electrical Engineering, Harbin University of Science and Technology in 2011, and the M.S. degree from the School of Mechanical Design, Harbin Institute of Technology, China, in 2013. where he is currently pursuing the Ph.D. degree. His research interests include electromechanical servo control, system identification, modeling and control of system, modeling and control of the parallel robot, and hardware-in-the-loop simulation.

JUNWEI HAN was born in Shenyang, Liaoning, China, in 1965. He received the B.S., M.S., and Ph.D. degrees in fluid power transmission and control system from the Harbin Institute of Technology, China, in 1986, 1989, and 1992, respectively. Since1997, he has been a Professor with the School of Mechatronics Engineering, Harbin Institute of Technology. His research interests include electro-hydraulic servo control and the key technology of large shaking table, and swing platform.

ZHIYONG QU was born in Yantai, Shandong, China, in 1978. He received the B.S., M.S., and Ph.D. degrees from the School of Mechatronics Engineering, Harbin Institute of Technology, China, in 1999, 2001, and 2006, respectively. He is currently an Associate Professor with the School of Mechatronics Engineering, Harbin Institute of Technology. He is also a member of the Institute of Electrohydraulic Servo Simulation and Test System, Harbin Institute of Technology. His research interests include modal analysis and control strategy of the redundant shaking table, and structure design and control strategy of the six degree of freedom system.

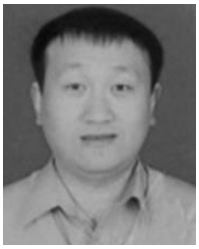

YU YANG was born in Shenyang, Liaoning, China, in 1980. He received the B.S., M.S., and Ph.D. degrees from the School of Mechatronics Engineering, Harbin Institute of Technology, China, in 2003, 2005, and 2010, respectively. He is currently a member of the Institute of Electrohydraulic Servo Simulation and Test System, Harbin Institute of Technology. His research interests include structure design and control strategy of the six degree of freedom systems, and the key technologies of flight simulator.